
Article:
Okujima, M., Yoshikawa, K., Mori, S. et al. (6 more authors) (2021) Molecular beam epitaxial growth of GaAs/GaNAsBi core–multishell nanowires. Applied Physics Express, 14 (11). 115002. ISSN 1882-0778

https://doi.org/10.35848/1882-0786/ac32a7

Molecular beam epitaxial growth of GaAs/GaNAsBi core–multishell nanowires

Masahiro Okujima†[1], Kohei Yoshikawa†[1], Shota Mori[1], Mitsuki Yukimune[1], Robert D. Richards[2], Bin Zhang[3], Weimin M. Chen[3], Irina A. Buyanova[3], Fumitaro Ishikawa*[1]

[1] Graduate School of Science and Engineering, Ehime University, 3 Bunkyo-cho, Matsuyama, Ehime, 790-8577, Japan

[2] Department of Electronic and Electrical Engineering, University of Sheffield, Broad Lane, Sheffield, S3 7HQ, United Kingdom

[3] Department of Physics, Chemistry and Biology, Linköping University, 58183 Linköping, Sweden

†These authors contributed equally to this work.

*Corresponding author email: ishikawa.fumitaro.zc@ehime-u.ac.jp

Abstract

GaAs/GaNAsBi/GaAs core–multishell nanowires were grown using molecular beam epitaxy on Si(111) substrates. The formation of the 20 nm-wide GaNAsBi shell with a regular hexagonal structure was observed. The shell is estimated to contain approximately 1.5% N and 2.6% Bi and has a compressive lattice mismatch of less than 0.2 % with GaAs layers. The strain mediation by the introduction of both N and Bi suppresses the crystalline deformation, resulting in the clear formation of the GaNAsBi shell. Thus, we obtained room-temperature photoluminescence with the maximum position at approximately 1300 nm from the GaAs/GaNAsBi/GaAs core–multishell nanowires.

III–V semiconductor nanowires (NWs) have attracted interest for various applications due to their superior electronic and optical properties.[1–3] Epitaxial heterostructured NWs can be grown on Si substrates, which shows the potential for their integration on the developed Si platform.[1–7] GaAs is a representative III-V semiconductor material employed for lasers and optical amplifiers operating in the near-infrared regime as well as in photovoltaics. Hence, the extension of the GaAs-based material's functions have potential for developing electronic systems that have not yet been realized. Dilute nitrides and bismides have been material systems of interest for decades.[8-10] A few percentage substitutions by these elements of group V As provide uncommon modifications of the band structure of the host matrix.[8-10] The covalent bond lengths of Ga–N and Ga–Bi are largely different and opposite to those of Ga–As. Hence, the quaternary GaNAsBi, which can form a heteroepitaxial layer with GaAs, provides great tunability of the band gap and lattice constants.[11,12] To date, by using self-catalyzed molecular beam epitaxy (MBE) on a Si(111) substrate we have produced GaNAs NWs which support laser operation,[13,14] and GaAsBi NWs which show specific structural modifications.[15-17] Both the constituent GaNAs and GaAsBi are metastable and the growth conditions strongly affect the morphology of the NWs.[11,18-21] The nanowires with clean facets, and well-defined Bi-containing regions were challenging to obtain for Bi-containing NWs because of the characteristic diffusion and segregation of Bi at the growth front[15-17]. Until now, GaAsBi NWs without strong deformation could only be fabricated with Bi concentrations of up to 1.2%[22]. The NWs with a Bi concentration over 2% and 1100 nm wavelength emission at room temperature (RT) showed large structural deformation.[15-17] Here, we report the molecular beam epitaxy (MBE) of GaAs/GaNAsBi/GaAs core–multishell heterostructure NWs, where the GaNAsBi shell containing 1% N and 3% Bi does not exhibit structural degradation and shows RT emission at 1300 nm.

The investigated samples were grown on phosphorous-doped n-type Si(111) substrates in a plasma-assisted MBE system.[13,16,17,23] A conventional solid-source effusion cell was

used to supply Ga. An as valved cracker cell was operated in As_4 mode. Nitrogen was supplied by an electron cyclotron resonance plasma source.[24] The surfaces of the epi-ready Si substrates were not treated prior to NW growth. The substrate surface was thus covered with a thin native oxide with a typical thickness of several nanometers. The pinholes in this oxide layer induced the formation of nanocraters, which acted as nucleation sites for the NWs.[23] The GaAs NW core was then formed by vapor–liquid–solid growth assisted by constituent Ga seed particles when Ga and As_4 flux were supplied to the Si substrate.[25,26]. We grew two series of GaAs/GaNAsBi/GaAs core–multishell samples using the following procedure. The beam equivalent pressure (BEP) of As_4 was adjusted to 6×10^{-4} Pa for the core and 1×10^{-3} Pa for the shells. The Ga supply was set to match a planar growth rate of 1 mL/s on GaAs(001) before growth. The atomic V/III ratio was 1 under these conditions. Bi BEP was set to 3.5×10^{-5} Pa for the growth. The GaAs core growth was initiated by opening the Ga shutter under an As overpressure and the GaAs core was grown for 30 min at 560 °C. By introducing a growth interruption and maintaining the As_4 flux, the Ga catalyst crystallized. The Ga flux was reduced to 0.5 ML/s planar growth equivalent during the crystallization. Subsequently, lateral growth became dominant, which was expected to form wire shells.[13,15] The first GaAs shell was grown for 20 min, followed by a second growth interruption. During the interruption, the growth temperature was reduced and the nitrogen plasma was ignited. The GaNAsBi shell was grown at a substrate temperature of 350 °C [15-17]. The N plasma was operated at 30 W with a N_2 flow rate of 0.7 sccm. The GaAs shell was then grown for 2 min, the GaNAsBi shell was grown for 3 min by opening the shutter of the plasma source, and the outermost GaAs shell was grown for 30 min. The nanowire formed a GaAs/GaNAsBi/GaAs core–shell structure.[15-17] Based on these growth parameters, the GaNAsBi shell was expected to form a 20 nm-wide layer. From the conditions of Bi BEP and nitrogen plasma operation, the Bi and N concentrations within the GaNAsBi layer were targeted to be approximately 3% and 1%, respectively. The atomic flux and the compositions of the GaNAsBi layer in the NWs were calibrated by growing planar

GaAs/GaNAsBi/GaAs heterostructures by placing a GaAs(001) substrate next to Si(111) on the Mo substrate holder block for growth, which provided good agreement for the compositions of the grown layers between the test sample and NWs in our previous study, [13-17, 27-29] even though the growth rate is different between those. From the X-ray diffraction of the thin film samples, we obtained the expected compositions of the GaNAsBi shell layer assuming identical compositions between the thin film and the NWs shell grown at in the vapor–solid mode.[13-17,27-29]

Structural characteristics of NWs were investigated using scanning electron microscopy (SEM) and cross-sectional scanning transmission electron microscopy (STEM). Axially sliced single NW samples for STEM investigation were prepared by focused ion beam processing (Helios660, FEI, USA). STEM was conducted on a single NW using a JEM-ARM200F Dual-X TEM microscope (JEOL, Japan) operating at 200 kV with energy dispersive X-ray spectrometry (EDS) employing a 100 mm^2 silicon drift detector (JED-2300, JEOL). STEM images were obtained in both bright-field (BF) and high-angle annular dark field (HAADF) modes, and fast Fourier transform (FFT) diffraction patterns were analyzed.[16,17] Photoluminescence (PL) measurements were performed using a micro-PL system at RT. PL excitation was conducted using a 660 nm solid-state laser at 3 mW. The PL signal was collected in a backscattering geometry through a 0.5 NA microscope objective and detected using a liquid nitrogen-cooled InGaAs charge-coupled device detector attached to a grating monochromator.

Figures 1 (a) and (b) show the plan-view and 30°-tilted SEM images of the NW sample. The NWs were found to have a typical length of 3–5 μm and an average diameter of 400 nm. The wires prefer vertical alignment with respect to the substrate surface with a vertical yield of approximately 70%. The wires have a spherical tip and roughened sidewall surface as observed in our previous study on GaAsBi NWs. This is induced by the surface diffusion of the Bi atoms at the growth front and the resultant morphological deformations as the previous reports. [15-17, 29]

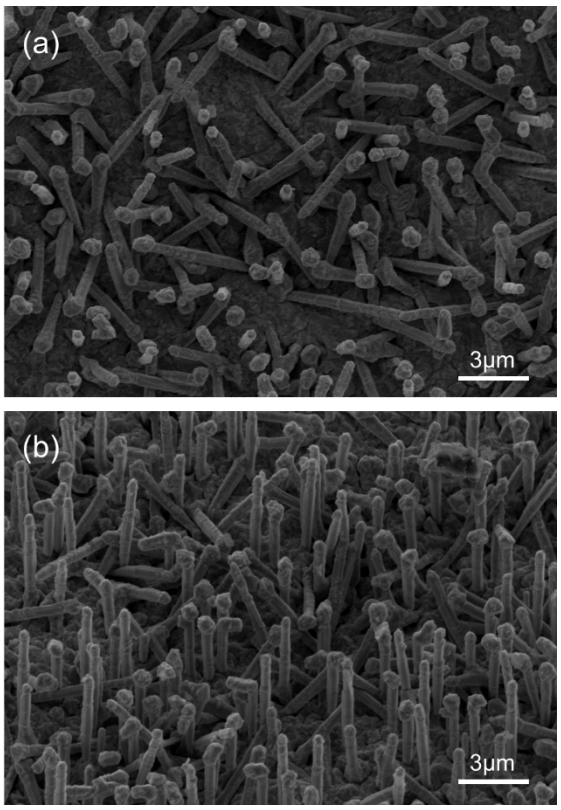

Figure 1. (a) Plan view and (b) 30°-tilted SEM images of the fabricated GaAs/GaNAsBi/GaAs core–multishell nanowires.

Figure 2 (a) and (b) show the axial cross-sectional BF-STEM and HAADF-STEM images of the GaAs/GaNAsBi/GaAs nanowire sample, respectively. The wire has a diameter of 400 nm and contains GaAs/GaNAsBi/GaAs core–shell layers. The dimensions of the corresponding layers can be estimated to be ~ 200 nm (the GaAs core), 20 nm (the width of the GaNAsBi shell), and 80 nm (the width of the outermost GaAs shell), which agrees well with the expected structure from the growth protocol.[13-17,27-29] The non-regular hexagonal sidewall structure of the outermost shell sidewall shown in Fig. 2(a) should be induced by the existence of residual Bi as reported in our previous study.[15-17] The Bi element is hard to be completely incorporated into the GaNAsBi matrix and the residual Bi diffuses on the growth front until its evaporation, resulting in the characteristic structural morphology in this materials

system.[15-17, 30] The GaNAsBi inner shell is clearly distinguished by the dark contrast in the BF image, as well as the bright contrast in the HAADF image in Fig. 2(b). The HAADF image provides information about the elemental distribution based on its Z-contrast image, where elements of larger atomic numbers exhibit a brighter contrast.[16,17] The bright contrast at the inner shell in Fig. 2(b) thus suggests the formation of the Bi-containing layers with the inclusion of a sufficient amount of Bi elements in the area.[16, 17, 30] As seen in the enlarged BF image in Fig. 2 (c), the GaAs/GaNAsBi inner interface is sharp. However, the outer GaNAsBi/GaAs interface can be recognized but is slightly dispersed compared to the inner interface. A sharp initial interface and roughening of the overlayer are often observed for the heterointerface of multi-elemental alloy systems such as these dilute nitrides, [31] where the accumulation of epitaxial strain or phase separation occurs.[32,33] In contrast, the atomic arrangement is well ordered and there is no structural degradation or contrast modulation for the GaNAsBi shell, as seen in the enlarged HAADF-STEM image in Fig. 2 (d). Hence, we conclude that the possible degradation induced by the strain accumulation and the phase separation are modestly suppressed in the GaNAsBi shell and do not critically degrade the layer, as seen in the cross-sectional images in Figs. 2(a) and (b). The FFT diffraction patterns shown in Fig. 4(c) obtained for the indicated areas of the GaNAsBi shell, GaAs core, and a spot at the outer GaNAsBi/GaAs interface are shown in Fig. 2 (e–g). Both patterns indicate that the vertices of the NW are directed to <112> between adjacent {110} side planes. The lattice distances for $(2\bar{2}0)$ and $(\bar{2}02)$ diffraction obtained from the FFT patterns of Fig. 2 (e-g) are 1.93 Å and 1.92 Å for the GaNAsBi shell, 1.92 Å and 1.92 Å for the GaAs core, and 1.93 Å and 1.92 Å for the outer interface, respectively. These results suggest that the GaNAsBi region is under approximately 0.2% compressive strain. Previously, we observed structural deformations by the introduction of Bi when it was introduced with concentrations exceeding 2%. Under these conditions, we observed strong structural deformation and the loss of regular hexagonal structure.[15-17] Consequently, the strain mediation in GaNAsBi by the introduction of both N and Bi at

appropriate concentrations enables a small lattice mismatch between GaAs and improves the GaNAsBi/GaAs heterointerface. EDS elemental mapping for Bi, Ga, and As shown in Figs. 2 (h), (i), and (j), respectively, confirm the formation of the Bi-containing inner shell. It is noteworthy that the detection of nitrogen intensity in EDS requires approximately 3% based on our previous study, and thus we cannot detect it due to the expected lower N concentration than that. [13,29] Therefore, the N distribution cannot be detected here because of the expected N concentration of about 1%. The quantitative analysis for the EDS elemental mapping provides the Bi concentration of 2.6% ± 0.3%. From the obtained lattice separation in the above diffraction pattern analysis, we obtained a lattice constant of 5.65-5.68 Å for the GaNAsBi layer, which is almost lattice matched to GaAs. Combining the diffraction pattern analysis and quantitative EDS, we can estimate the Bi and N concentration at the GaNAsBi layer to be 2.6% for Bi and about 1.5% for N with errors of about ± 0.3%.[20,34]

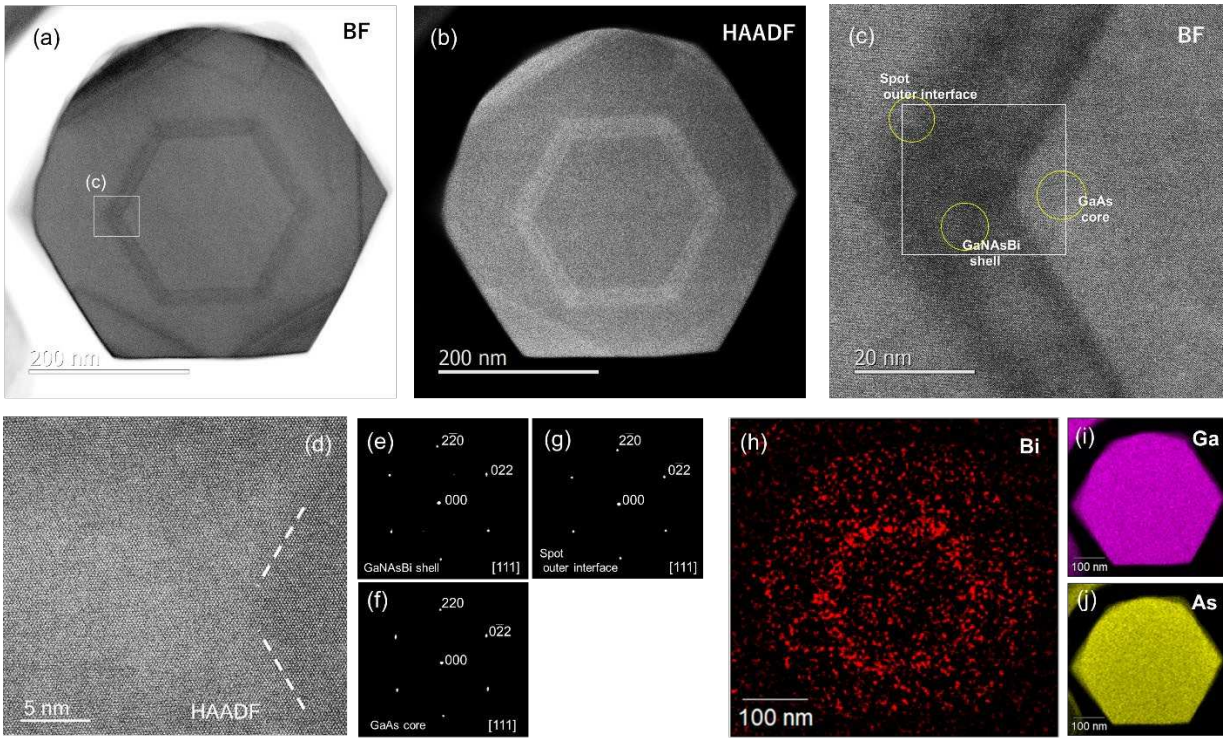

Figure 2. Results of axial cross-sectional STEM-EDS investigations of GaAs/GaNAsBi/GaAs core–multishell structure. (a) BF-STEM and (b) HAADF-STEM image. (c) Higher magnification BF-STEM image at the area delimited by the rectangle in (a) and (d) further higher magnification HAADF-STEM image at the area delimited by the rectangle in (c). FFT diffraction patterns observed from the [111] direction at the areas of (e) GaNAsBi shell, (f) GaAs core, and (g) the spot at the outer interface as indicated in (c) . The dashed lines shown in (d) indicate the GaNAsBi/GaAs interface extracted from the contrast difference. EDS elemental mapping of (h) Bi, (i) Ga, and (j) As.

Figure 3 shows the RT PL spectrum measured from the ensemble of the GaAs/GaNAsBi/GaAs core–multishell NWs. The detected emission has maximum intensity at 1300 nm. This ensemble spectral position is consistent with 2.6% Bi and 1.5% N,[35] as estimated from the EDS results on the individual NW in Fig. 2. This suggests that the luminescence originates from band-to-band transitions within the NW GaNAsBi shells. We

note that quantum confinement effects are not expected to affect the transitions energy due to the relatively large thickness (20 nm) of the shell. The observed significant broadening of the PL spectrum could be due to fluctuations of the alloy composition commonly seen in Bi-containing alloys,[20] as well as structural variations within the nanowire ensemble.

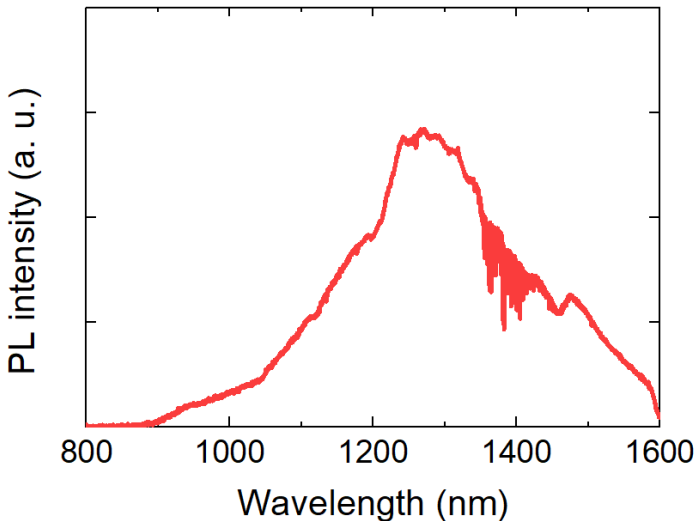

Figure 3. Room-temperature PL spectrum of GaAs/GaNAsBi/GaAs core–multishell NW ensemble.

In summary, we have grown GaAs/GaNAsBi/GaAs core–multishell nanowires by self-catalyzed MBE on a Si(111) substrate. The nanowires, grown at 350 °C, show a regular hexagonal GaNAsBi shell with a width of 20 nm. Based on the cross-sectional STEM-EDS studies, the shell was estimated to contain approximately 1.5% N and 2.6% Bi, showing a lattice mismatch of less than 0.2%, with the low strain appearing to suppress lattice deformation. Thus, we obtained RT photoluminescence at approximately 1300 nm from the GaAs/GaNAsBi/GaAs core–multishell nanowire ensemble. Our results, therefore, show that co- alloying with Bi and N results in high structural and optical quality of GaNAsBi NWs, promising for future applications of this material system in nanoscale light emitters operating in the infrared regime.

Acknowledgments

This work was partly supported by KAKENHI (No. 16H05970, 19H00855, and 21KK0068) from Japan Society of Promotion of Science. The work of RDR was supported by the Royal Academy of Engineering under the Research Fellowships scheme. IB would like to acknowledge the financial support from the Swedish Research Council (Grant No. 2019-04312). IB and WMC acknowledge financial support from the Swedish Government Strategic Research Area in Materials Science on Functional Materials at Linköping University (Faculty Grant SFO-Mat-LiU No 2009 00971).

References

[1] M. S. Gudiksen, L. J. Lauhon, J. Wang, D. C. Smith, C. M. Lieber, Nature 415, 617 (2002).

[2] H. Zhang, C.-X. Liu, S. Gazibegovic, D. Xu, J. A. Logan, G. Wang, N. van Loo, J. D. S. Bommer, M. W. A. de Moor, D. Car, R. L. M. Op het Veld, P. J. van Veldhoven, S. Koelling, M. A. Verheijen, M. Pendharkar, D. J. Pennachio, B. Shojaei, J. S. Lee, C. J. Palmstrøm, E. P. A. M. Bakkers, S. Das Sarma, L. P. Kouwenhoven, Nature 556, 74 (2018).

[3] Novel Compound Semiconductor Nanowires: Materials, Devices, and Applications, edited by F. Ishikawa and I. A. Buyanova (Pan Stanford Publishing, Singapore (2017).

[4] K. Tomioka, M. Yoshimura, T. A. Fukui, Nature 488, 189 (2012).

[5] M. T. Björk, C. Thelander, A. E. Hansen, L. E. Jensen, M. W. Larsson, L. R. Wallenberg, L. Samuelson, Nano Lett. 4, 1621 (2004).

[6] X. Miao, K. Chabak, C. Zhang, P. K. Mohseni, D. Walker, Jr., X. Li, Nano Letters, 15, 2780 (2015).

[7] B. Zhang, Y. Huang, J. Eric Stehr, P.-P. Chen, X.-J. Wang, W. Lu, W. M. Chen, I. A. Buyanova, Nano Lett., 19, 6454 (2019).

[8] Ed. M. Henini, Dilute Nitride Semiconductors, (Elsevier Science, Amsterdam, 2005.)

[9] Eds. I. Buyanova and W. Chen, Physics and Applications of Dilute Nitrides, (Taylor and Francis, New York, 2004).

[10] Eds. S. Wang, P. Lu, *Bismuth-Containing Alloys and Nanostructures,* (Springer, Singapore, 2019).

[11] M. Yoshimoto, W. Huang, Y. Takehara, J. Saraie, A. Chayahara, Y. Horino, K. Oe, Jpn. J. Appl. Phys. 43, L845 (2004).

[12] M. Yoshimoto, W. Huang, G. Feng, K. Oe Phys. Stat. Solidi B, 243, 1421 (2006).

[13] M. Yukimune, R. Fujiwara, H. Ikeda, K. Yano, K. Takada, M. Jansson, W. Chen, I. Buyanova, F. Ishikawa, Appl. Phys. Lett. 113, 011901 (2018).

[14] S. Chen, M. Yukimune, R. Fujiwara, F. Ishikawa, W. M. Chen, I. A. Buyanova, Nano Letters, 19, 885 (2019).

[15] F. Ishikawa, Y. Akamatsu, K. Watanabe, F. Uesugi, S. Asahina, U. Jahn, S. Shimomura, Nano Lett. 15, 7265, 2015.

[16] T. Matsuda, K. Takada, K. Yano, R. Tsutsumi, K. Yoshikawa, S. Shimomura, Y. Shimizu, K. Nagashima, T. Yanagida, F. Ishikawa, Nano Lett., 19, 8510 (2019).

[17] T. Matsuda, K. Takada, K. Yano, S. Shimomura, Y. Shimizu, F. Ishikawa, Appl. Phys. Lett., 117, 113105 (2020).

[18] J. C. Harmand, G. Ungaro, L. Largeau, G. Le Roux, Appl. Phys. Lett. 77, 2482 (2000).

[19] J. E. Stehr, R. M. Balagula, M. Jansson, M. Yukimune, R. Fujiwara, F. Ishikawa, W. M. Chen, I. A. Buyanova, Nanotechnology 31, 065702 (2020).

[20] L. Wang, L. Zhang, L. Yue, D. Liang, X. Chen, Y. Li, P. Lu, J. Shao, S. Wang, Crystals, 7, 63, 2017.

[21] X. Lu, D. A. Beaton, R. B. Lewis, T. Tiedje, M. B. Whitwick, Appl. Phys. Lett. 92, 192110 (2008).

[22] T. Matsuda, K. Takada, K. Yano, S. Shimomura, F. Ishikawa, J. Appl. Phys., 125, 194301 (2019).

[23] J. H. Paek, T. Nishiwaki, M. Yamaguchi, and N. Sawaki, Phys. Status Solidi (c) **6,** 1436 (2009).

[24] M. Yoshikawa, K. Miura, Y. Iguchi, Y. Kawamura, J. Cryst. Growth **311** 1745 (2009).

[25] A. Fontcuberta i Morral, C. Colombo, G. Abstreiter, J. Arbiol, J. R. Morante Appl. Phys. Lett. **92** 063112 (2008).

[26] B. Mandl, J. Stangl, E. Hilner, A. A. Zakharov, K. Hillerich, A. W. Dey, L. Samuelson, G. Bauer, K. Deppert, A. Mikkelsen Nano Lett. **10** 4443 (2010).

[27] Y. Araki, M. Yamaguchi, F. Ishikawa, Nanotechnology, 24, 065601 (2013).

[28] N. Ahn, Y. Araki, M. Kondow, M. Yamaguchi, F. Ishikawa, Jpn. J. Appl. Phys., 53, 065001 (2014).

[29] M. Yukimune, R. Fujiwara, T. Mita, N. Tsuda, J. Natsui, Y. Shimizu, M. Jansson, R. Balagula, W. M. Chen, I. A. Buyanova, F. Ishikawa, Nanotechnology, 30, 244002 (2019).

[30] J. A. Steele, R. A. Lewis, J. Horvat, M. J. B. Nancarrow, M. Henini, D. Fan, Y. I. Mazur, M. Schmidbauer, M. E. Ware, S.-Q. Yu, G. J. Salamo, Sci. Rep. 6, 28860 (2016).

[31] X. Wu, M. D. Robertson, J. A. Gupta, and J. M. Baribeau J. Phys.: Condens. Mater. 20, 075215 (2008).

[32] F. Ishikawa, E. Luna, A. Trampert, K. H. Ploog., Appl. Phys. Lett. 89, 181910 (2006).

[33] Trampert, J.-M. Chauveau, K. H. Ploog, E. Tournié, and A. Guzmán, J. Vac. Sci. Technol. B 22, 2195 (2004).

[34] I. Vurgaftman, J. R. Meyer, J. Appl. Phys. 94, 3675 (2003).

[35] S. Sweeney, K. Hild, S. Jin, In 2013 IEEE 39th Photovoltaic Specialists Conference, 2474-2478 (2013).